TISSUE ENGINEERING

Protein-releasing polymeric scaffolds induce fibrochondrocytic differentiation of endogenous cells for knee meniscus regeneration in sheep

Chang H. Lee,[1] Scott A. Rodeo,[2] Lisa Ann Fortier,[3] Chuanyong Lu,[1] Cevat Erisken,[1] Jeremy J. Mao[1]*

Regeneration of complex tissues, such as kidney, liver, and cartilage, continues to be a scientific and translational challenge. Survival of ex vivo cultured, transplanted cells in tissue grafts is among one of the key barriers. Meniscus is a complex tissue consisting of collagen fibers and proteoglycans with gradient phenotypes of fibrocartilage and functions to provide congruence of the knee joint, without which the patient is likely to develop arthritis. Endogenous stem/progenitor cells regenerated the knee meniscus upon spatially released human connective tissue growth factor (CTGF) and transforming growth factor–β3 (TGFβ3) from a three-dimensional (3D)–printed biomaterial, enabling functional knee recovery. Sequentially applied CTGF and TGFβ3 were necessary and sufficient to propel mesenchymal stem/progenitor cells, as a heterogeneous population or as single-cell progenies, into fibrochondrocytes that concurrently synthesized procollagens I and IIα. When released from microchannels of 3D-printed, human meniscus scaffolds, CTGF and TGFβ3 induced endogenous stem/progenitor cells to differentiate and synthesize zone-specific type I and II collagens. We then replaced sheep meniscus with anatomically correct, 3D-printed scaffolds that incorporated spatially delivered CTGF and TGFβ3. Endogenous cells regenerated the meniscus with zone-specific matrix phenotypes: primarily type I collagen in the outer zone, and type II collagen in the inner zone, reminiscent of the native meniscus. Spatiotemporally delivered CTGF and TGFβ3 also restored inhomogeneous mechanical properties in the regenerated sheep meniscus. Survival and directed differentiation of endogenous cells in a tissue defect may have implications in the regeneration of complex (heterogeneous) tissues and organs.

INTRODUCTION

The meniscus in the knee joint is a crescent-shaped connective tissue between the distal femoral and proximal tibial condyles that provides structural congruence and absorbs mechanical forces (*1*). Meniscus injuries are treated with meniscus resection with or without a cadaveric meniscus graft (*2*). Meniscectomy exposes femoral and tibial condyles to excessive wear and is a highly predisposing factor for osteoarthritis, the most prevalent cause of chronic disabilities among heart failure, spinal cord injuries, respiratory disorders, and stroke (*1*). Meniscus replacement with allografts or cadaveric tissue suffers from limited graft availability, pathogen transmission, immune rejection, and anatomical mismatch (*1*, *2*). Injuries and diseases of all fibrocartilage tissues, including the meniscus, the tendon-bone junctions, the intervertebral discs of the spine, and the temporomandibular joint, fail to heal spontaneously, leading to collective health care burden estimated in multiple billions of dollars annually in the United States alone (*1*, *3*).

A seemingly insurmountable obstacle in meniscus regeneration, similar to the regeneration of most other complex tissues, is the paucity of viable cells capable of regenerating multiple tissue phenotypes (*1*). Heterogeneous populations of connective tissue cells constitute the meniscus including fibroblast-like cells primarily in the outer zone with abundant collagen type I, whereas the inner zone primarily consists of chondrocyte-like cells rich in sulfate glycosaminoglycans (GAGs) and collagen type II (*1*, *5*). The intermediate zone contains fibrochondrocytes, a cell type that produces both type I and type II collagens (*1*, *5*). Previous work on meniscus regeneration has revealed that no single-cell source is sufficient to regenerate heterogeneous meniscus tissues (*1*, *6*). Furthermore, the meniscus is devoid of vascular supply except for the outer zone. The perceived deficiency of vascular-derived stem/progenitor cells is considered a hurdle in meniscus regeneration (*2*).

Two acellular biomaterials cleared for human use in Europe appear to relieve pain and symptoms but have yielded inconsistent clinical outcome and reported adverse events including graft shrinkage, problematic attachment and integration into host tissue, and myxoid degeneration (*4*, *5*). Absent in previous work on the regeneration of the meniscus is fibrocartilage phenotype that needs to be restored for proper meniscus function to withstand both tensile and compressive stresses (*4*, *5*). The regenerated meniscus tissue should not only restore cell and matrix properties but also perform mechanical functions, analogous to other efforts to regenerate the heart, lungs, kidney, bladder, and bone (*7*–*10*).

Here, we have devised a three-dimensional (3D)–printed, anatomically correct biomaterial scaffold that can coax endogenous cells to regenerate the meniscus with fibrocartilage tissues in specific zones. The scaffold releases two human proteins in a spatially and temporally controlled manner, leading to the generation of multiple tissue phenotypes, yielding instructive clues for the regeneration of complex tissues in a translational model. The present protein delivery approach seems readily poised for a human clinical trial in which proteins are packaged in a good manufacturing practice (GMP) facility and shipped to hospitals and clinics for patient use.

RESULTS

Sequential growth factor treatment induces fibrochondrocyte differentiation of human mesenchymal stem/progenitor cells in vitro

We first derived fibrochondrocyte-like cells—meniscus-resident cells that concurrently produced both type I and type II collagens—from human

[1]Tissue Engineering and Regenerative Medicine Laboratory, Columbia University Medical Center, New York, NY 10032, USA. [2]Department of Orthopaedic Surgery, Hospital for Special Surgery, 525 East 71st Street, New York, NY 10021, USA. [3]Department of Clinical Sciences, College of Veterinary Medicine, Cornell University, Ithaca, NY 14853, USA.
*Corresponding author. E-mail: jmao@columbia.edu

bone marrow and synovium mesenchymal stem/progenitor cells (MSCs) in vitro. Sequential application of recombinant human connective tissue growth factor (rhCTGF) for 2 weeks in culture, followed by recombinant human transforming growth factor–β3 (rhTGFβ3) for 2 weeks (C→T in Fig. 1 and fig. S1), induced differentiation of MSCs into cells that synthesized procollagens I and IIα, suggesting that they were fibrochondrocyte-like cells, with a yield of 72.22% in monolayer culture and 76.92% in 3D fibrin hydrogels. This yield for C→T was significantly higher than that for the reverse (T→C) and the combination (T+C), both in monolayer culture and in 3D fibrin (Fig. 1A and table S1) (Student's *t* test: $P < 0.000001$ for C→T versus T→C; $P = 0.0032$ for C→T versus T+C). C4 or T4 alone failed to yield fibrochondrocyte-like cells. MSC differentiation into fibrochondrocyte-like cells was attenuated upon reversed sequential treatment with TGFβ3 and CTGF (T→C) or either CTGF (C4) or TGFβ3 (T4) alone (Fig. 1A and table S1).

MSCs treated with C→T demonstrated significantly higher *collagen I*, *collagen II*, and *aggrecan* mRNA than the control (untreated MSCs) (Fig. 1, B to D, and table S2). Moreover, C→T not only induced MSC differentiation but also yielded a fibrocartilaginous matrix that stained positively for picrosirius red and alcian blue in both monolayer culture (fig. S2A) and 3D fibrin gels (fig. S3A), indicating synthesis of both type I and type II collagens, respectively. C→T treatment led to greater GAG

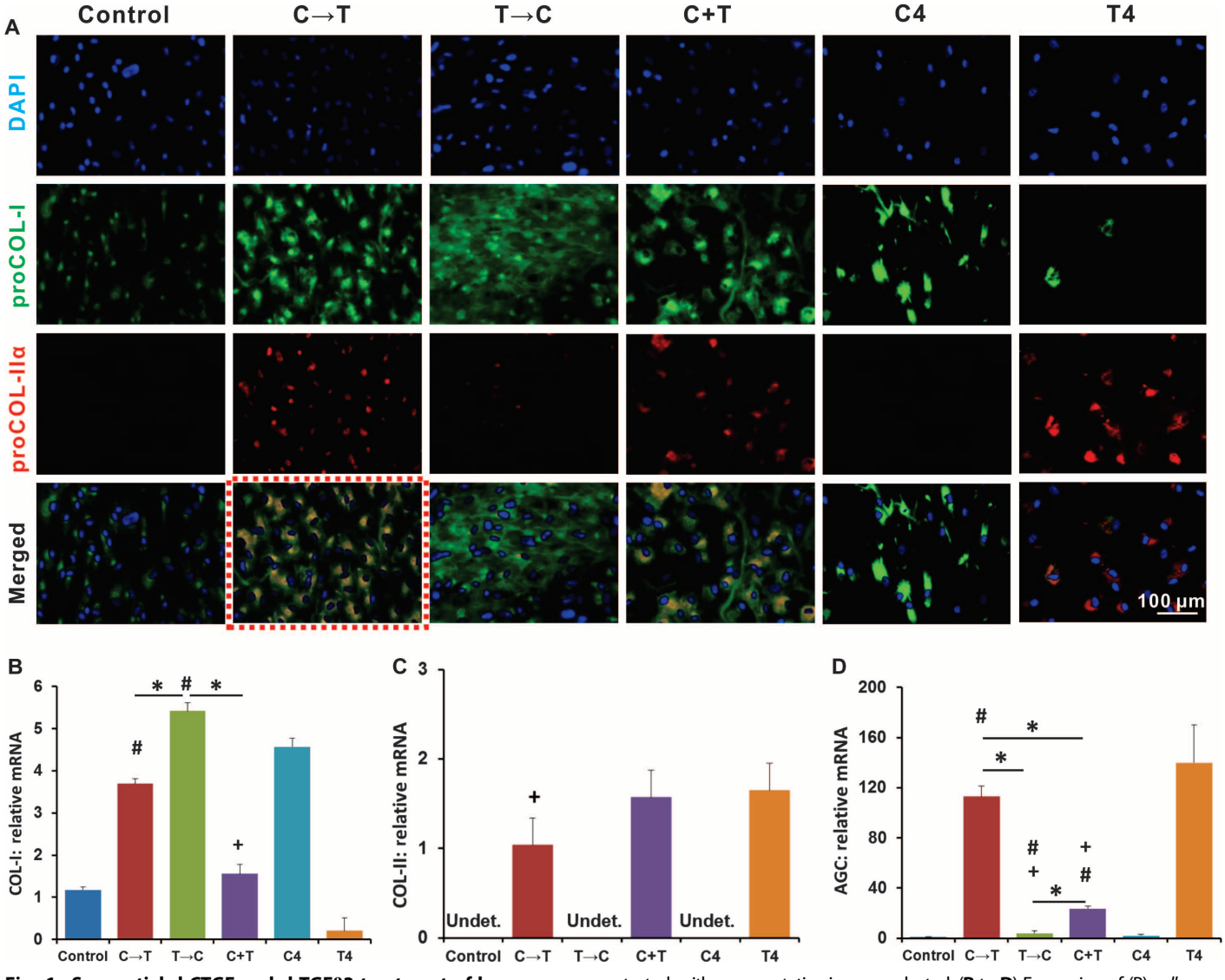

Fig. 1. Sequential rhCTGF and rhTGFβ3 treatment of bone marrow MSCs induces fibrochondrocyte differentiation. (**A**) Immunofluorescence analysis of procollagen I chain (proCOL-I) and procollagen IIα (proCOL-IIα) production by human MSCs treated in culture with C→T (rhCTGF for 2 weeks followed by rhTGFβ3 for 2 weeks), T→C (rhTGFβ3 for 2 weeks followed by rhCTGF for 2 weeks), C+T (rhCTGF and TGFβ3 concurrently for 4 weeks), C4 (rhCTGF alone for 4 weeks), and T4 (rhTGFβ3 alone for 4 weeks). Cell nuclei were stained with 4′,6-diamidino-2-phenylindole (DAPI). A total of five replicates were tested, with representative images selected. (**B** to **D**) Expression of (B) *collagen type I* (COL-I), (C) *collagen type II* (COL-II), and (D) *aggrecan* (AGC) mRNA after MSC exposure to treatments in (A), with the exception that concurrent CTGF and TGFβ3 application (C+T) was 4 weeks. Data are averages ± SD ($n = 5$) normalized to *GAPDH*, then relative to control. $^{*}P < 0.05$ between indicated groups; $^{\#}P < 0.05$ versus control; $^{+}P < 0.05$ versus positive control (C4 for *collagen type I* or T4 for *collagen type II* and *aggrecan*), one-way analysis of variance (ANOVA) with post-hoc Tukey's B test. Complete statistical analysis is in table S2.

content than T→C (figs. S2B and S3B), but T→C produced more type II collagen than did C→T (figs. S2C and S3C). However, T→C failed to yield a substantial number of fibrochondrocyte-like cells, thus making this treatment approach unlikely for meniscus regeneration in vivo (Fig. 1). We found that C→T elevated collagen I expression by fibrochondrocytes primarily via focal adhesion kinase (FAK) signaling, whereas collagen II and aggrecan expression was driven primarily via p38 signaling (fig. S4). Collectively, sequential application of rhCTGF and rhTGFβ3 was necessary and sufficient to induce fibrochondrogenic differentiation of human MSCs in vitro.

MSCs isolated as mononucleated and adherent cells from bone marrow and other sources are heterogeneous, and typically represent a mix of mature cells such as osteoblasts, fibroblasts, and some stem/progenitor cells. We therefore performed clonal analysis to ascertain that fibrochondrocytes were derived from progenies of a single MSC. Of 59 randomly selected MSCs from human bone marrow, 29 (~53%) yielded clonal progenies, such as A5, B6, D7, and H1 (fig. S5A), by limiting dilution. About 55% of clonal progenies, including A5 and B6, differentiated into fibrochondrogenic, osteogenic, chondrogenic, and adipogenic cells in corresponding chemically defined medium (fig. S5B). Together, MSCs, as a heterogeneous population or as single-cell progenies, can differentiate into cells that concurrently produce type I and II collagens, arguably fibrochondrocytes upon sequential CTGF and TGFβ3 application, signifying the need for in vivo testing of fibrocartilage regeneration.

3D printing fabricated human and sheep meniscus scaffolds

We chose to test the dynamic combination of CTGF and TGFβ3 in an established knee meniscus injury model (*11*, *12*), owing to its potential generalizability in the regeneration of complex, inhomogeneous tissues. Anatomically correct human meniscus scaffolds were fabricated using 3D printing (*13*). Briefly, poly-ε-caprolactone (PCL) was molten to fabricate an anatomically correct meniscus scaffold modeled after a reconstructed human cadaver meniscus (Fig. 2A). The 3D-printed human meniscus scaffold was at ~40% of the real size of a human cadaver meniscus (Fig. 2A), so that it fits in a cell culture well for additional experiments. Interlaid strands and interconnecting microchannels (diameters of 100 to 200 μm) were aligned along the circumferential direction as conduits for cellular ingrowth, mimicking the predominant meniscal collagen orientation (Fig. 2A, inset) (*14*) and allowing for cells to be metabolically satisfied [within 200 μm of blood vessels, as shown in (*15*)].

rhCTGF and rhTGFβ3 were microencapsulated in PLGA μS, with rhCTGF in 50:50 PLA/PGA μS and rhTGFβ3 in 75:25 PLA/PGA μS (Fig. 2B). CTGF and TGFb3 μS were tethered to the outer and inner regions of the meniscus scaffold, respectively. Physical bonding between protein-encapsulating μS and PCL microfibers was induced by ethanol. To validate multiphase μS distribution, fluorophore-conjugated dextrans with molecular weights similar to rhCTGF (~40 kD) and rhTGFβ3 (~10 kD) were delivered to the scaffold's outer and inner zones, respectively, at day 1 (Fig. 2C). At day 8, the distribution of 40-kD dextrans (green) and 10-kD dextrans (red) was maintained. Spheres with 50:50 ratio showed controlled release of CTGF first, followed by TGFβ3. Relatively rapid rhCTGF release from the outer layer and slower release of rhTGFβ3 from the inner layer were sustained over 42 days (Fig. 2D).

Before in vivo application of the growth factor–loaded PCL scaffold, we ascertained whether spatiotemporal delivery of rhCTGF and rhTGFβ3 induced zone-specific MSC differentiation into cells that produced type I and II collagens. Porous meniscus scaffolds incorporating rhCTGF and rhTGFβ3 for spatiotemporally controlled release were placed atop monolayer-cultured human synovium MSCs. After a 6-week incubation period in vitro, spatiotemporally released rhCTGF and rhTGFβ3 induced zone-specific expression of collagen types I and II, presumably from the differentiated synovium MSCs, with resemblance to the native rat meniscus (Fig. 2E). Abundant collagen type I was present primarily in the outer zone (picrosirius red–positive), whereas cartilaginous matrix with collagen type II was primarily in the inner zone (alcian blue–positive) (Fig. 2F). A mixed fibrocartilaginous matrix developed in the intermediate zone (Fig. 2F).

Spatially released CTGF and TGFβ3 from 3D-printed scaffolds led to regeneration of sheep knee meniscus

We aimed to regenerate the sheep meniscus in vivo by spatiotemporal release of rhCTGF and rhTGFβ3 in anatomically correct PCL scaffolds. Sheep is a widely used preclinical model for meniscus regeneration owing to its similarity to humans in vascular supply, anatomy, and biochemical composition (*16*). The native sheep medial meniscus was laser-scanned for the fabrication of total or partial meniscus scaffold (Fig. 3A), followed by spatial rhCTGF and rhTGFβ3 incorporation as described above.

Before in vivo implantation, the scaffold's internal microstructure was optimized to yield mechanical properties similar to those of the native sheep meniscus. Among 50- to 500-μm interlaid strands and interstrand microchannels, diameters of 200 and 100 μm were selected because they yielded dynamic compressive modulus (E^*), storage modulus (E'), and loss modulus (E'') similar to the intermediate zone of the native sheep meniscus (Fig. 3B). Pull-out tests were performed in harvested sheep cadavers after partial meniscectomy and suture fixation (fig. S6). The maximum pull-out strength of the scaffold-to-outer rim of the native meniscus was significantly higher than the native partial meniscus grafts-to-outer rims (54.5 N versus 39.8 N) (Fig. 3C and fig. S6). The equilibrium friction coefficient on angular velocity (0.01 to 1 rad/s) of the optimized scaffold was similar to the native meniscus (Fig. 3D).

A total of 11 skeletally mature (2- to 5-year-old) sheep were randomly allocated into control (scaffold only with empty μS; $n = 4$) and treatment (spatiotemporal rhCTGF and rhTGFβ3 delivery; $n = 7$) groups. We used partial meniscus grafting (Fig. 3A) owing to high clinical rates of partial meniscectomy (*1*, *2*). Anatomically correct meniscus scaffolds were implanted after partial meniscectomy (Fig. 3E). Briefly, the medial meniscus was exposed after femoral condylectomy. With all ligaments preserved, ~80% medial meniscus was resected including the inner, intermediate, and a major portion of the outer zone, followed by replacement with anatomically correct partial meniscus scaffolds. The meniscus scaffold was sutured to the remaining ~20% outer rim of the native meniscus. Twelve weeks after implantation, the scaffold integrated fully into the remaining outer rim of the meniscus, with no notable damage to articular cartilage in either the femoral or tibial condyle (Fig. 3F).

The native sheep meniscus showed a characteristic pattern of extracellular matrix distribution with fibroblast-like cells among collagen bundles in the outer zone, cartilage-like tissue in the inner zone, and a mixed fibrous and cartilage tissue in the intermediate zone (Fig. 4A). Spatiotemporal delivery of CTGF and TGFβ3 from the implanted scaffolds yielded native-like fibrocartilage: a collagen-rich, aligned fibrous matrix in the outer zone; a fibrocartilaginous matrix in the intermediate zone; and a cartilaginous matrix in the inner zone (Fig. 4B), resembling the zonal matrix characteristics of the native sheep meniscus.

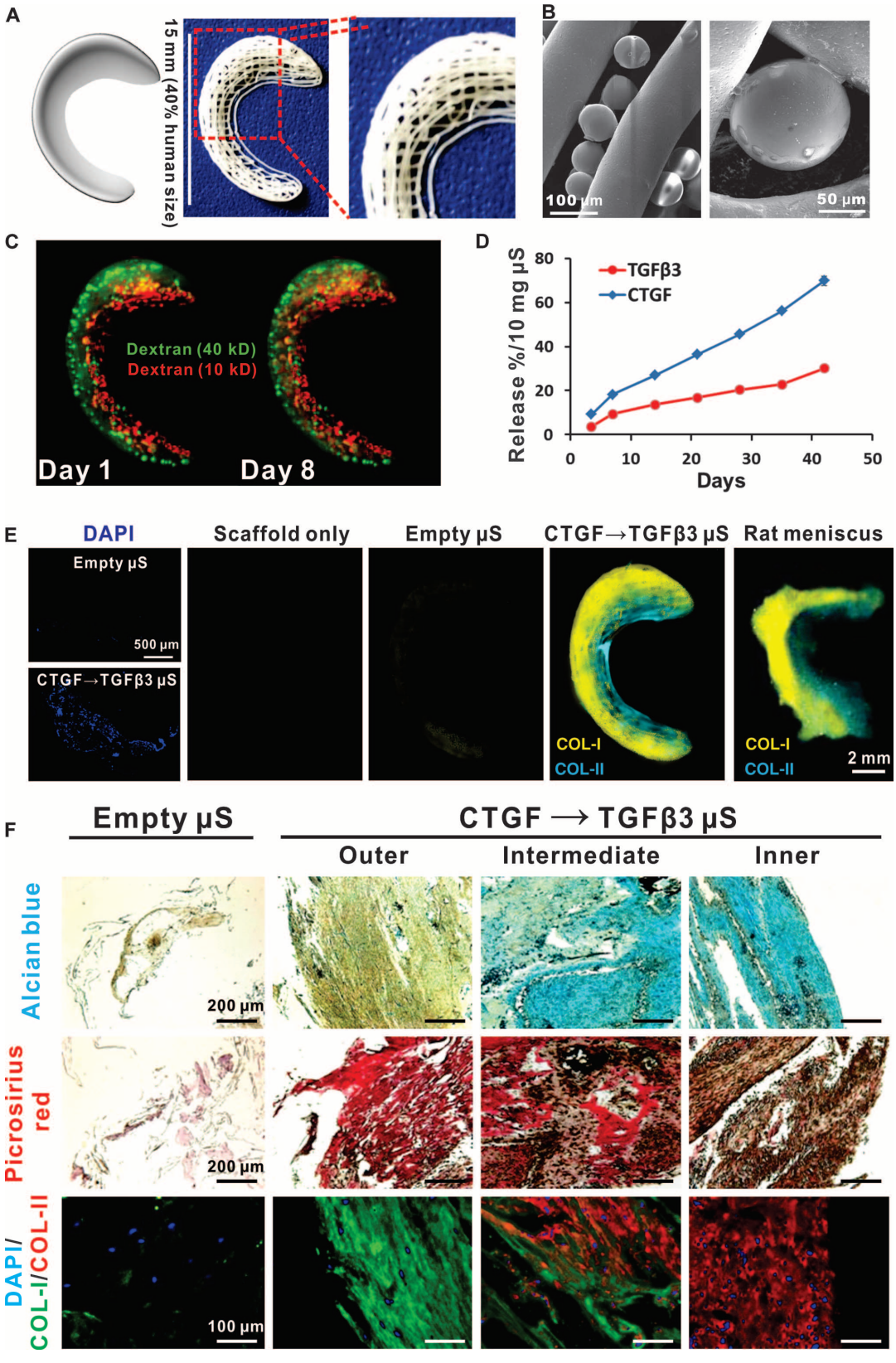

Fig. 2. Spatiotemporally released rhCTGF and rhTGFβ3 induced fibrocartilage-like matrix formation in 3D-printed porous scaffolds. (**A**) Anatomic reconstruction of human meniscus. Human meniscus scaffolds were 3D-printed with layer-by-layer deposition of PCL fibers (100-μm diameter), forming 100- to 200-μm channels. (**B**) Poly(lactic-*co*-glycolic acid) (PLGA) microspheres (μS) encapsulating rhCTGF and rhTGFβ3 were in physical contact with PCL microfibers. (**C**) Fluorescent dextrans simulating CTGF (green, 40 kD) and TGFβ3 (red, 10 kD) were delivered into the outer and inner zones, respectively, of human meniscus scaffolds to show scaffold loading. Distribution of dextrans was maintained from day 1 to day 8. (**D**) rhCTGF and rhTGFβ3 release from the PCL scaffolds over time in vitro. (**E**) When the scaffolds were incubated atop human synovium MSC monolayers for 6 weeks, spatiotemporally delivered rhCTGF and rhTGFβ3 induced cells to form zone-specific collagen type I and II matrices, similar to the native rat meniscus. (**F**) Scaffold with empty μS showed little matrix formation after 6 weeks of coculture with 1:1 mixture of fibrogenic and chondrogenic supplements (no growth factors in medium). Spatiotemporal delivery of rhCTGF and rhTGFβ3 induced fibrocartilaginous matrix formation, consisting of alcian blue–positive, collagen II–rich cartilaginous matrix in the inner zone and picrosirius red–positive, collagen I–rich fibrous matrix in the outer zone. A total of five replicates were tested, with representative images selected from the same scaffold.

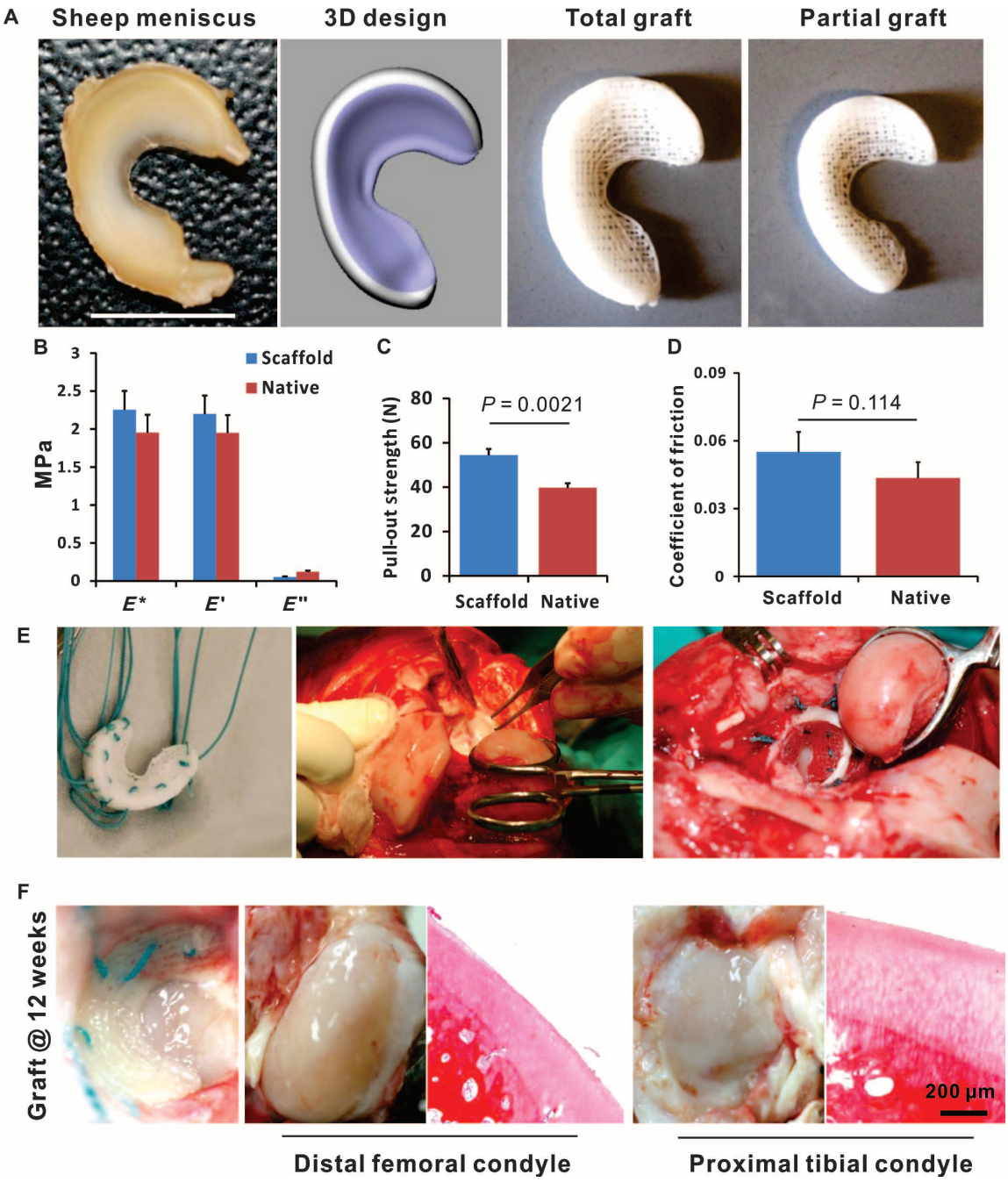

Fig. 3. Scaffold implantation in sheep meniscus in vivo is shown. (**A**) Anatomic contour of the medial meniscus was obtained from 3D laser scanning of a sheep cadaver meniscus and reconstructed in 3D. Anatomically correct meniscus scaffolds were fabricated for total or partial grafts by layer-by-layer deposition of PCL using 3D printing. Scale bar, 15 mm. (**B**) Dynamic modulus (*E**), storage modulus (*E'*), and loss modulus (*E''*) of PCL scaffolds with preoptimized internal microstructure (200-μm microstrands and 100-μm microchannels) compared with the native meniscus. (**C**) Suture pull-out strength in scaffold-to-native meniscus outer rim, sutured with 2-0 Ethibond. (**D**) Equilibrium friction coefficient of the scaffold, measured under steady frictional shear compared with the native meniscus. Data in (B) to (D) are means ± SD (n = 5). P values in (B) to (D) were determined by one-way ANOVA (n = 5 per group). (**E**) A scaffold was prepared for implantation with 2-0 Ethibond suture. The sheep medial meniscus was exposed by dislocating femoral condyle, followed by scaffold implantation. (**F**) After 12 weeks, the implanted scaffold from (E) fully integrated. Articular cartilages on femoral and tibia condyles showed little damage on hematoxylin and eosin (H&E) staining.

Sheep menisci replaced with anatomically correct scaffolds encapsulating empty μS showed amorphous fibrous tissue throughout, without zone-specific tissue phenotypes (Fig. 4C).

The regenerated meniscus tissue showed zone-specific cell phenotypes similar to the native meniscus (Fig. 4D). The outer zone of the regenerated meniscus was populated by fibroblast-like, spindle-shaped

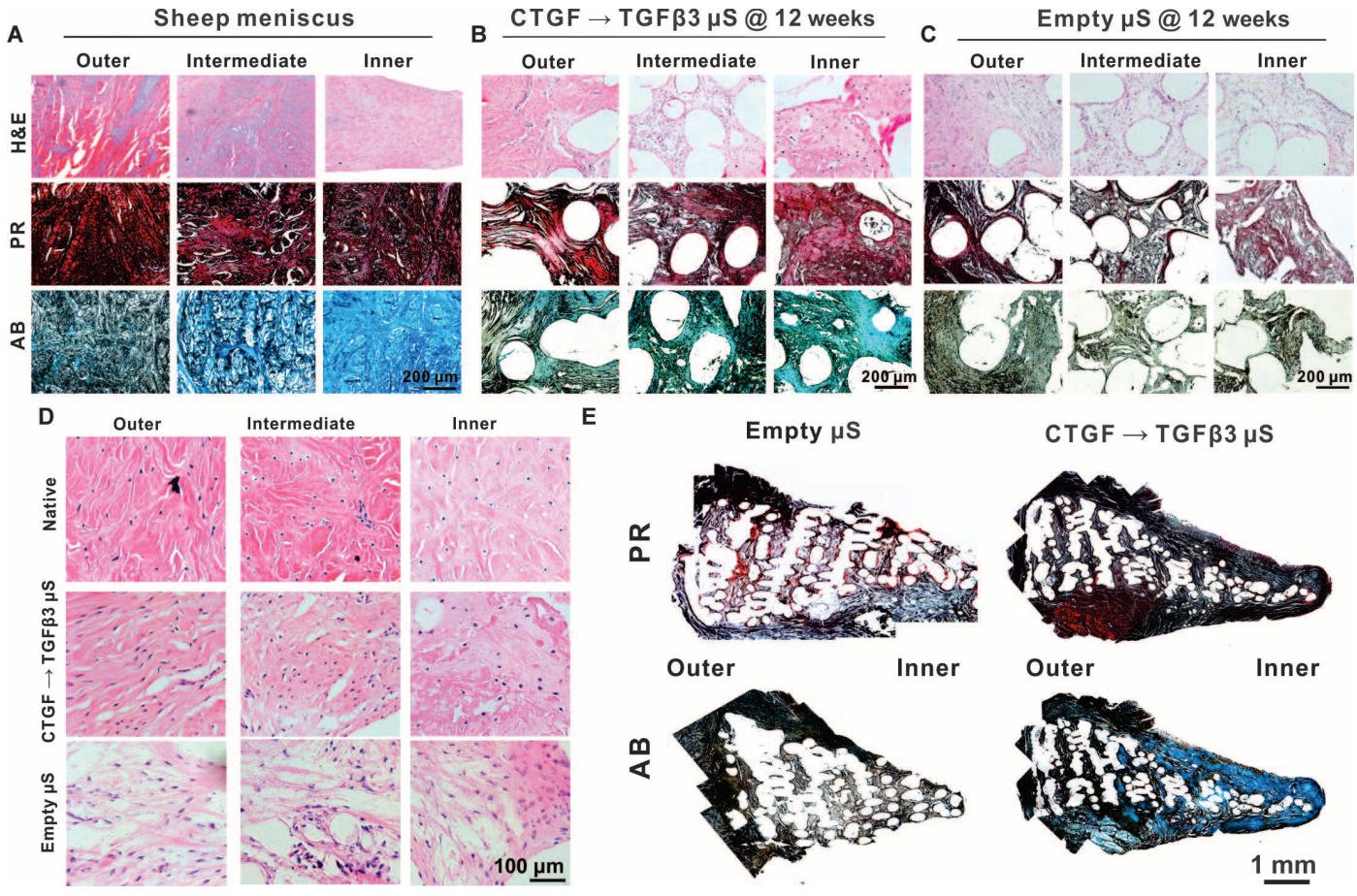

Fig. 4. Sheep meniscus regeneration and quality of the regenerated tissue are shown. (**A**) Distribution of fibrous and cartilage matrix in the native sheep meniscus. (**B** and **C**) After 12 weeks in vivo, zone-specific distribution in the spatiotemporally released rhCTGF and rhTGFβ3 group (B) compared with the control group (scaffolds with empty μS) (C). Tissue sections were stained for H&E, alcian blue (AB) (aggrecan), and picrosirius red (PR) (collagens I and III). (**D**) Outer, intermediate, and inner zone phenotypes of cells populating the regenerated meniscus (H&E staining). (**E**) Low-magnification images of retrieved meniscus grafts with spatiotemporal delivery of rhCTGF and rhTGFβ3 in comparison to empty μS after 12-week in vivo implantation. Images are representative of $n = 4$ for empty μS and $n = 7$ for C→T scaffolds.

cells; chondrocyte-like cells in the inner zone; and mixed fibroblast- and chondrocyte-like cells in the intermediate zone. Low-magnification images confirmed the presence of multiphase fibrocartilage throughout the scaffolds (Fig. 4E).

The regenerated knee meniscus restored biomechanical and functional properties

All sheep undergoing operation resumed weight bearing and locomotion as early as 3 weeks after surgery. A sheep that received a CTGF→TGFβ3 μS–laden scaffold in the medial meniscus of the left knee demonstrated fully restored locomotion and weight bearing at 6 weeks post-op (movie S1), whereas a sheep that received an anatomically correct scaffold but with empty μS is shown in movie S2. Both sheep were able to resume locomotion and weight bearing. However, CTGF→TGFβ3 delivery not only yielded zone-specific fibrocartilage tissue phenotype (Fig. 4B) but also restored mechanical properties of the regenerated fibrocartilage tissue.

Instantaneous modulus (E_i), relaxation modulus (E_r), and viscosity (μ) were measured by fitting to a Kelvin solid viscoelastic model (*17*, *18*). E_i, E_r, and μ of the native meniscus showed inhomogeneity along the radial zone, which includes the outer, intermediate, and inner zones of meniscus (Fig. 5), likely owing to multiphase distribution of collagen and GAGs in the meniscus (*17*, *18*). The CTGF→TGFβ3 delivery group yielded E_i, E_r, and μ similar to the native meniscus [$P > 0.05$, one-way ANOVA; post-hoc least significant difference (LSD)] (Fig. 5A). Contrastingly, the viscoelastic properties of the empty μS group were inferior to those of the CTGF→TGFβ3 μS group or the native menisci (Fig. 5A).

Young's modulus and ultimate strength from tensile testing at 1%/s (*17*) were significantly higher in the CTGF→TGFβ3 scaffold group and the native menisci than in the empty μS group (Fig. 5B). The ultimate strain showed no significant differences between the regenerated and native menisci (Fig. 5B).

DISCUSSION

These findings show that meniscus regeneration with inhomogeneous tissue properties and functional recovery is possible with a protein-releasing,

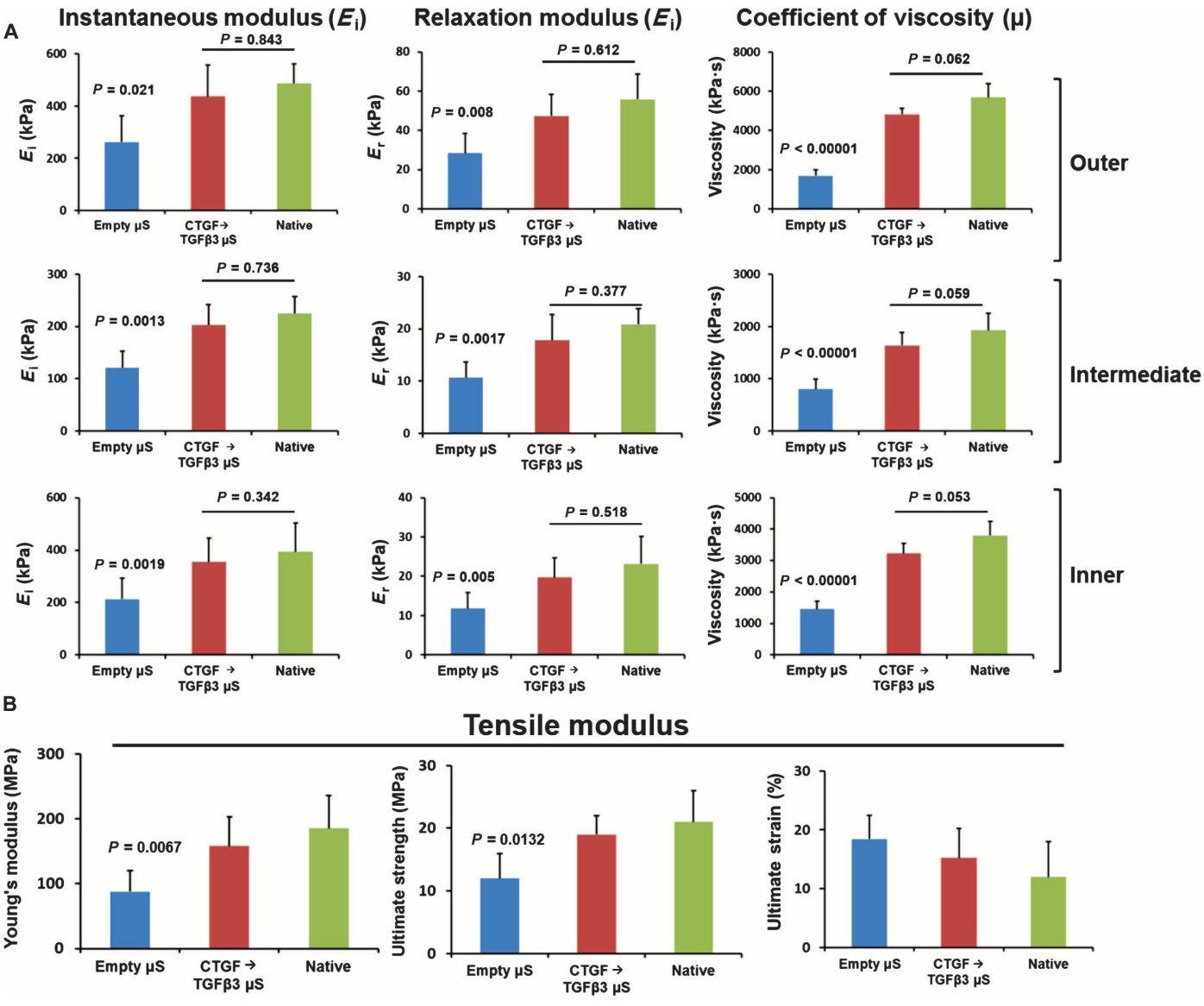

Fig. 5. Viscoelastic properties of the regenerated meniscus after 12 weeks. (**A**) Instantaneous modulus (E_i), relaxation modulus (E_r), and coefficient of viscosity (μ) were measured from stress-relaxation tests. E_i, E_r, and μ of the native meniscus in outer, intermediate, and inner zones were measured and compared with those of regenerated menisci. (**B**) Young's modulus and ultimate strength of the regenerated menisci by rhCTGF and rhTGFβ3 delivered from the scaffold compared with the empty μS. Data in (A) and (B) are means ± SD (n = 4 animals per group). P values for empty μS are compared with C→T (one-way ANOVA with post-hoc LSD).

acellular biomaterial scaffold. In contrast to cell transplantation, the present strategy of endogenous regeneration upon spatiotemporal release of two recombinant human proteins offers a ready-to-implant graft that may serve as a therapeutic prototype. Regeneration by cell homing, now being sporadically demonstrated in several tissue/organ systems (*12*, *13*, *19*), provides an alternative to cell transplantation. Biologically, regeneration by cell transplantation or cell homing is not mutually exclusive. Transplanted cells secrete cytokines that promote the survival, cell recruitment, or differentiation of host endogenous cells (*20*). However, regeneration by cell homing circumvents the need for ex vivo cell culture. Endogenous cells that have migrated to a healing wound are likely those with the ability to survive in situ. Contrastingly, en mass transplanted cells are exposed to an environment that may not be primed for cell vitality (*20*, *21*). Further, transplantation of parenchymal cells, which is typical of all cell delivery approaches, must rely on the recruitment of endogenous stromal cells for the generation of a complete tissue. Recently, growth factor binding was shown to be a primary mechanism of action of fibrin in diabetic wound repair without cell transplantation (*22*).

How recruited endogenous cells, including stem/progenitor cells, or transplanted parenchymal cells orchestrate stromal as well as vascular, neural, lymphatic, and immune components in a restored tissue warrants

further investigation. Here, a fibrochondrocyte phenotype was derived from MSCs when CTGF and TGFβ3 were sequentially applied in vitro or spatiotemporally released in vivo. FAK and p38 pathways have been implicated in collagen and aggrecan synthesis, and hence were studied here. Our initial data suggest that C→T elevates *collagen I* mRNA expression primarily via FAK signaling, whereas *collagen II* and *aggrecan* mRNA expression was increased primarily via p38 signaling. Such preliminary signaling studies could yield clues for additional targets in enhancing meniscus regeneration.

Despite precise and reproducible in vitro CTGF and TGFβ3 release kinetics that led to fibrochondrogenic phenotype, in vivo actions of released proteins and peptides are best judged by the quality of the tissue they are intended to regenerate (*23*, *24*), in this case, a consistent yield of fibrocartilage in vivo. Meniscus regeneration demands not only restoration of biological structures at cell and matrix levels but also the capacity to exert mechanical functions, analogous to the regeneration of the heart, lungs, kidney, bladder, and blood vessels (*7*–*9*). Inhomogeneity is characteristic of many biological tissues and all organs. No previous reports to our knowledge have shown functional regeneration or restoration of heterogeneous meniscal tissue phenotypes (*16*, *25*–*29*), although some studies have shown partial healing with somewhat homogeneous tissue or pain relief in large animal models or patients (*4*, *5*).

The present study reports regeneration of an inhomogeneous, functional knee meniscus in a large animal model with 3-month follow-up. Longer-term evaluation will be needed to assess whether zone-specific tissue phenotypes are sustained with daily function. Our previous work showed reconstitution of a single, uniform tissue—albeit fibrous tissue—by in vivo delivery of CTGF alone (*12*) or articular cartilage upon in vivo delivery of TGFβ3 alone (*13*). Cell sources for the observed meniscus regeneration may derive from synovium stem/progenitor cells in the wound (*30*) and also from the remaining ~20% native, vascularized meniscus tissue (*2*), suggesting that perhaps vascular-derived stem/progenitor cells are recruited by appropriate molecules. Previous work has shown the validity of dual growth factors in the formation of a singular neovascular network (*31*).

A drawback of a large animal model is its impossibility to delineate cell sources by cell tracing/tracking approaches that are available in transgenic mice (*32*). The sheep model also does not permit broad immunophenotyping of regenerated tissues owing to a paucity of antibodies and probes. Although we were unable to track cell recruitment in the sheep, host cell recruitment was demonstrated in a 50% rat meniscus resection defect when $LacZ^+$ cells in BMP7-treated Achilles tendon allograft were transplanted (*33*, *34*), which supports our hypothesis of meniscus regeneration by endogenous cells.

For translation, we envision a 3D-printed human meniscus-shaped material scaffold where both recombinant human proteins, rhCTGF and rhTGFβ3, are tethered in the scaffold's microchannels and packaged in a GMP/GLP (good laboratory practice) facility. The packaged products are shipped to hospitals and clinics where meniscus replacement surgeries are performed. The surgeons replace injured menisci using the existing arthroscopy procedure with an off-the-shelf meniscus scaffold rather than the current allograft from cadaver meniscus. Reproducible derivation of fibrochondrocytes from postnatal MSCs by CTGF and TGFβ3 may have broad implications in the regeneration of other fibrocartilage tissues, including the intervertebral disc of the spine, the tendon-bone junction, and the temporomandibular joint, each of which, when diseased, is a severe health care burden.

METHODS

Study design

The overall objective and design of the study was to determine whether endogenous cells, including stem/progenitor cells, can be differentiated in situ to regenerate complex tissues, specifically the knee meniscus. The primary parameters of study design included (i) extracellular matrix synthesis and expression of aggrecan, GAGs, and collagen types I and II, which collectively are macromolecules in the native meniscus; (ii) clonogenicity of bone marrow and synovium MSCs; (iii) differentiation capacity of bone marrow and synovium MSCs at population and clonal levels; (iv) mechanical properties of scaffold material including pull-out tests; and (v) mechanical properties of regenerated tissues.

The ability of the acellular, growth factor–releasing material to regenerate fibrocartilage was investigated in vivo in an ovine model. A power analysis was performed before our preclinical, large animal study, as described below. The original sample size was five for the control group and eight for the treated group. A total of 13 sheep were operated on, with 11 reaching end points ($n = 4$ for control; $n = 7$ for treated). Two sheep were lost because of anesthesia and surgical complications. The treatment was randomized and blinded from team members who performed the surgeries and postsurgical care. End points were predefined as the presence or absence of statistically significant differences of the above-listed parameters. No outliers were eliminated.

MSC isolation and fibrochondrogenic differentiation

Human MSCs were isolated from commercially available, fresh whole bone marrow samples or surgically removed synovium of anonymous adult donors (age range, 20 to 25 years) per our previous methods (*12*, *13*). Passage 2/3 MSCs (100,000 cells per well) were plated in six-well culture plates, or 3D pellets were formed by centrifuging 2×10^6 MSCs in 15-ml conical tubes. Monolayered cells or cell pellets were treated with (i) CTGF (100 ng/ml) (BioVendor) for 2 weeks followed by TGFβ3 (10 ng/ml) (R&D Systems) (C→T); (ii) TGFβ3 (10 ng/ml) for 2 weeks followed by CTGF (100 ng/ml) for 2 weeks (T→C); (iii) mixture of CTGF (100 ng/ml) and TGFβ3 (10 ng/ml) for 4 weeks (C+T); or (iv) CTGF for 4 weeks (C4), TGFβ3 for 4 weeks (T4), and growth medium as a control (Fig. 1). Fibrochondrogenic induction supplement [ascorbic acids (50 μg/ml)] and chondrogenic induction supplements [1% 1× ITS+1 solution, sodium pyruvate (100 μg/ml), L-ascorbic acid 2-phosphate (50 μg/ml), L-proline (40 μg/ml), 0.1 μM dexamethasone] were included in the CTGF and TGFβ3 treatments, respectively (*12*).

After 4 weeks of treatment, harvested samples (monolayers and pellet sections) were stained with alcian blue and picrosirius red per our previous methods (*12*). GAGs and types I and II collagen were quantitatively assayed (Biocolor) and normalized to DNA content (*12*). Immunofluorescence was performed to identify cells expressing proCOL-I (ab64409) and/or proCOL-IIα (ab17771), both from Abcam.

Cellular cloning

MSC clones were established by limiting dilution (*12*). Briefly, passage 0 MSCs were suspended at a concentration of one cell per 200 μl and seeded in 96-well plates with 200 μl of regular growth medium per well. After 24 hours, wells with only one cell were marked (fig. S5) and maintained in culture at 37°C and 5% CO_2, with medium change every 3 to 4 days. After 3 to 4 weeks, single-cell–derived clonal progenies were treated with 0.25% trypsin-EDTA and seeded into 24-well plates. Clonal progenies were transferred to six-well plates upon ~80% confluence and

maintained with medium change every 3 to 4 days. Established clones were induced for multilineage differentiation into osteogenic, chondrogenic, and adipogenic lineages per our previous methods (*12*), and fibrochondrogenic lineage as described above (fig. S5).

Design and synthesis of anatomically correct meniscus scaffolds

Anatomically correct meniscus scaffolds were fabricated using 3D-Bioplotter (EnvisionTEC) per our previous work (*13*). Briefly, the anatomic contour of the medial meniscus of human or skeletally mature sheep was captured by multislice laser scanning and reconstructed by computer-aided design. PCL (molecular weight, ~65,000; Sigma) was molten at 120°C and dispensed, following the layer path dictated by 3D design of internal microstructures. For the human meniscus scaffold, interlaid strands and interconnecting microchannels had a diameter of 100 μm, and circumferentially aligned fibers were added to recapitulate predominant collagen orientation in the native meniscus (Fig. 2A). For the sheep meniscus scaffold (Fig. 3A), 300-μm microstrands and 100-μm microchannels were determined to be optimal (Fig. 3A) to approximate mechanical properties of the native meniscus.

Spatiotemporal CTGF and TGFβ3 delivery

Recombinant human CTGF and TGFβ3 were encapsulated in 50:50 and 75:25 (PLA/PGA) μS, respectively, using double emulsion (*12*). Two different PLGA ratios were applied to yield controlled CTGF and TGFβ3 release. Briefly, a total of 250 mg of PLGA was dissolved into 1 ml of dichloromethane. CTGF (10 μg) or TGFβ3 (2.5 μg) was diluted to 50 μl following the manufacturer's protocols and added to the PLGA solution, forming a mixture (primary emulsion) that was emulsified for 1 min (water-in-oil). The primary emulsion was then added to 2 ml of 1% polyvinyl alcohol (PVA; molecular weight, 30,000 to 70,000), followed by 1-min mixing [(water-in-oil)-in-water]. Upon adding 100 ml of PVA, the mixture was stirred for 1 min at room temperature. A total of 100 ml of 2% isopropanol was added to the final emulsion and continuously stirred for 2 hours to remove the solvent. Control microspheres (empty, without CTGF or TGFβ3, reflecting a mixture of both 75:25 and 50:50 PLA/PGA) were fabricated with 50 μl of distilled water. Release kinetics of CTGF and TGFβ3 from PLGA μS were measured by incubating microspheres (10 mg/ml) encapsulating CTGF [in phosphate-buffered saline (PBS)] or TGFβ3 (0.1% bovine serum albumin) at 37°C with mild agitation for up to 42 days (*12*). Upon centrifugation at 2500 rpm for 5 min, supernatant of the PLGA μS incubation solution was collected. Released CTGF and TGFβ3 concentration was measured using enzyme-linked immunosorbent assay (ELISA) kits following the manufacturer's protocols.

PLGA μS (10 mg/ml) containing either CTGF or TGFβ3 were then incorporated on scaffold's microstrands by ethanol treatment for 1 hour (*35*). CTGF-encapsulated μS were applied in the microchannels in the scaffold's outer/middle zones, whereas TGFβ3-encapsulated μS were applied in inner/middle zones. Multiphase distribution of CTGF and TGFβ3 μS was validated by incorporating μS-encapsulating fluorescein-conjugated dextran (40 kD) and Alexa Fluor 546 dextran (10 kD), representing CTGF and TGFβ3, respectively. Dextran distribution was visualized using Maestro (PerkinElmer). Upon fibrin gel infusion into microchannels, scaffolds with dextran-encapsulated μS were incubated at 37°C for 8 days and imaged with Maestro.

In vitro cell recruitment and tissue synthesis

The anatomically correct meniscus scaffolds with spatiotemporal delivery of CTGF-TGFβ3 were placed on top of monolayer cultured human synovium MSCs (100,000 per well) in a six-well plate. After 6 weeks of culture with a mixture of fibrogenic and chondrogenic supplemented medium, the scaffolds were harvested and analyzed for cell recruitment and zone-specific tissue formation. Cell recruitment was confirmed by DAPI staining in the scaffolds, and tissue formation was evaluated by histology and immunofluorescence.

Meniscectomy and grafting

A total of 11 sheep were randomly allocated into treated (n = 7) and control (n = 4) groups. A medial parapatellar approach was made through the skin and subcutaneous tissue. A lateral parapatellar arthrotomy was performed, and the patella was luxated medially. After flexing of the joint and exposure of the medial meniscus, condylectomy was performed using an oscillating saw from the axial side of the medial femoral condyle toward the distal medial femoral metaphysis. All the associated joint ligaments were preserved. Then, a partial meniscectomy was performed by resecting all but ~20% of the meniscus' outer zone and immediately grafted with anatomically correct meniscus scaffold, followed by suturing (2-0 Ethibond Excel, Braided). Condylectomy was repaired with 2- or 4.5-mm-diameter cortical bone screws. The joint capsule and subcutaneous tissue were closed separately in continuous absorbable suture. The skin was staple-closed and covered with a sterile bandage.

The operated sheep were confined to small pens (4 × 4 ft^2) to minimize sudden or extended movements. Sheep were in direct visual, vocal, and nasal contact with each other, but were in separate pens to minimize inadvertent trauma. Pain medication (narcotics and nonsteroidal anti-inflammatory drugs) was administered intramuscularly for a minimum of 2 weeks post-op. Upon complete condylectomy healing on radiographs, sheep were group-housed in a small paddock (six sheep per 12 × 12 ft^2 paddock) for 1 week for acclimation and then transferred to a large paddock (96 × 96 ft^2) until euthanasia. All in vivo samples were harvested at 12 weeks post-op. Harvested tissue was fixed in 4% formaldehyde, embedded in paraffin, and cut in 5-μm sections.

Mechanical tests

Four of seven treated samples were selected for mechanical testing. The other three samples were used for tissue-based analyses.

Dynamic compression. Before in vivo implantation, dynamic compression was performed to match scaffold's mechanical properties with those of the native meniscus (*13*). Briefly, cylindrical plugs were punched from the central regions of scaffolds and native meniscus (5 × 5 mm^2) (n = 5 per group). Compressive testing was performed under 10% cyclic strain at 2 Hz, and dynamic compressive properties were characterized as complex compressive modulus E^*, storage modulus E', and loss modulus E''. All mechanical tests were performed using ElectroForce BioDynamic testing system (Bose).

Pull-out strength. About 75% of the sheep medial meniscus was longitudinally cut with a scalpel. A total of four holding sutures (2-0 Ethibond Excel, Braided) were placed between the inner and outer portions of the meniscus and the scaffold. The maximum pull-out force was measured after mounting the samples using stainless steel wired on ElectroForce tensile grips and pulled at 0.5 mm/s (*36*).

Friction coefficient. Equilibrium friction coefficients, μeq, on angular velocity were measured to estimate the scaffold's frictional property (*19*). Cylindrical samples (10-mm diameter × 3-mm thickness), prepared from the middle region of menisci and scaffolds, were fixed to an impermeable bottom platen using cyanoacrylate glue and immersed

in a PBS bath. After 5% compressive tare strain for 1800 s, a series of sequential angular velocities (0.01, 0.1, and 1 rad/s) were applied for 120 s each. Friction coefficient (μ_{eq}) was calculated as friction force (F) divided by normal force (N). With an assumption of zero unknown frictional shear at the center and linear distribution along with the radial direction, the average frictional force, F, was obtained as $F = 4T/3r_0$, where T is the frictional torque and r_0 was the specimen's radius.

Stress relaxation. Disc-shaped samples (5-mm diameter × 2-mm thickness) were prepared from the inner, middle, and outer regions of the native and regenerated menisci. Using unconfined compression, samples were preconditioned with 15 cycles of 0 to 5% compressive strain, followed by stress relaxation with 20% compressive strain. A Kelvin standard solid viscoelastic model was applied to calculate instantaneous modulus (E_i), modulus of relaxation (E_r), and viscosity (μ) (*19*, *24*).

Tensile test. Circumferential strips of the middle region of the native and regenerated menisci were cut into dog bone shapes 25 mm in length and 1 mm in average thickness per previous methods (*19*, *24*). After preconditioning of 15 cycles of 0 to 2% strain, tensile tests were performed at 1% strain per second. The linear portion of each stress-strain curve was used to determine the Young's modulus (E_y). The ultimate strength and strain was determined from each curve.

Data analysis and statistics

Sample sizes for all quantitative data were determined by power analysis with one-way ANOVA using an α level of 0.05, power of 0.8, and effect size of 1.50 chosen to assess matrix synthesis, gene expressions, and mechanical properties in the regenerated meniscus tissues and controls upon verification of normal data distribution. In case of skewed data distribution, a nonparametric test, Kruskal-Wallis one-way ANOVA, will be performed using an α level of 0.05, power of 0.8, and effect size of 1.50. Analysis using PASS (NCSS) indicated necessary sample sizes of four to seven to achieve a power value of 0.8 for the in vitro and in vivo parameters used in the present study. Expected SD and means were entered on the basis of our previous work for meniscus tissue regeneration and MSC differentiations (*13*). Briefly, f analysis was performed with estimated means and SDs of control and test groups using the following equation:

$$f = \sqrt{\sum_{i=1}^{k} \frac{p_i \times (\mu_i - \mu)^2}{\sigma^2}}$$

where $p_i = n_i/N$; n_i = number of observation in group i; N = total number of observations; μ_i = estimated mean of group i; μ = grand mean; σ^2 = error variance within the group. For all quantitative data, one-way ANOVA with post-hoc LSD or Tukey's B tests were used.

SUPPLEMENTARY MATERIALS

www.sciencetranslationalmedicine.org/cgi/content/full/6/266/266ra171/DC1

Fig. S1. Fibrochondrogenic differentiation of human bone marrow MSCs in 3D fibrin.

Fig. S2. Fibrochondrogenic matrix production by fibrochondrocytes derived from human MSCs in monolayer culture.

Fig. S3. Fibrochondrogenic matrix production by fibrochondrocytes derived from human MSCs in 3D fibrin gel.

Fig. S4. FAK and p38 signaling plays a role in collagen and aggrecan expression after fibrochondrocyte differentiation in vitro.

Fig. S5. Single-cell progenies of human bone marrow MSCs differentiate into fibrochondrocytes.

Fig. S6. Mechanical testing of scaffold to meniscus and partially resected meniscus.

Table S1. Fibrochondrocyte differentiation from human bone marrow MSCs in monolayer and 3D cultures.

Table S2. Statistical significances for comparisons in between groups in Fig. 1, fig. S2, and fig S3.

Movie S1. Sheep movement after medial meniscus replacement with 3D-printed scaffold with spatial CTGF and TGFβ3 delivery.

Movie S2. Sheep movement after medial meniscus replacement with 3D-printed scaffold with empty μS.

REFERENCES AND NOTES

1. K. A. Athanasiou, J. Sanchez-Adams, *Engineering the Knee Meniscus* (Morgan and Claypool Publishers, San Rafael, CA, 2009).
2. F. R. Noyes, S. D. Barber-Westin, Repair of complex and avascular meniscal tears and meniscal transplantation. *J. Bone Joint Surg. Am.* **92**, 1012–1029 (2010).
3. Centers for Disease Control and Prevention Report (2011); http://www.cdc.gov/mmwr/preview/mmwrhtml/mm5601a2.htm.
4. D. M. O'Halloran, A. S. Pandit, Tissue-engineering approach to regenerating the intervertebral disc. *Tissue Eng.* **13**, 1927–1954 (2007).
5. H. S. Cheung, Distribution of type I, II, III and V in the pepsin solubilized collagens in bovine menisci. *Connect Tissue Res.* **16**, 343–356 (1987).
6. B. M. Baker, R. L. Mauck, The effect of nanofiber alignment on the maturation of engineered meniscus constructs. *Biomaterials* **28**, 1967–1977 (2007).
7. A. Atala, S. B. Bauer, S. Soker, J. J. Yoo, A. B. Retik, Tissue-engineered autologous bladders for patients needing cystoplasty. *Lancet* **367**, 1241–1246 (2006).
8. J. Kajstura, M. Rota, S. R. Hall, T. Hosoda, D. D'Amario, F. Sanada, H. Zheng, B. Ogórek, C. Rondon-Clavo, J. Ferreira-Martins, A. Matsuda, C. Arranto, P. Goichberg, G. Giordano, K. J. Haley, S. Bardelli, H. Rayatzadeh, X. Liu, F. Quaini, R. Liao, A. Leri, M. A. Perrella, J. Loscalzo, P. Anversa, Evidence for human lung stem cells. *N. Engl. J. Med.* **364**, 1795–1806 (2011).
9. H. C. Ott, T. S. Matthiesen, S. K. Goh, L. D. Black, S. M. Kren, T. I. Netoff, D. A. Taylor, Perfusion-decellularized matrix: Using nature's platform to engineer a bioartificial heart. *Nat. Med.* **14**, 213–221 (2008).
10. J. J. Song, J. P. Guyette, S. E. Gilpin, G. Gonzalez, J. P. Vacanti, H. C. Ott, Regeneration and experimental orthotopic transplantation of a bioengineered kidney. *Nat. Med.* **19**, 646–651 (2013).
11. P. Bianco, X. Cao, P. S. Frenette, J. J. Mao, P. G. Robey, P. J. Simmons, C. Y. Wang, The meaning, the sense and the significance: Translating the science of mesenchymal stem cells into medicine. *Nat. Med.* **19**, 35–42 (2013).
12. C. H. Lee, B. Shah, E. K. Moioli, J. J. Mao, CTGF directs fibroblast differentiation from human mesenchymal stem/stromal cells and defines connective tissue healing in a rodent injury model. *J. Clin. Invest.* **120**, 3340–3349 (2010).
13. C. H. Lee, J. L. Cook, A. Mendelson, E. K. Moioli, H. Yao, J. J. Mao, Regeneration of the articular surface of the rabbit synovial joint by cell homing: A proof of concept study. *Lancet* **376**, 440–448 (2010).
14. A. C. Abraham, C. R. Edwards, G. M. Odegard, T. L. Donahue, Regional and fiber orientation dependent shear properties and anisotropy of bovine meniscus. *J. Mech. Behav. Biomed. Mater.* **4**, 2024–2030 (2011).
15. R. K. Jain, P. Au, J. Tam, D. G. Duda, D. Fukumura, Engineering vascularized tissue. *Nat. Biotechnol.* **23**, 821–823 (2005).
16. H. Katagiri, T. Muneta, K. Tsuji, M. Horie, H. Koga, N. Ozeki, E. Kobayashi, I. Sekiya, Transplantation of aggregates of synovial mesenchymal stem cells regenerates meniscus more effectively in a rat massive meniscal defect. *Biochem. Biophys. Res. Commun.* **435**, 603–609 (2013).
17. F. T. Moutos, F. Guilak, Functional properties of cell-seeded three-dimensionally woven poly(ε-caprolactone) scaffolds for cartilage tissue engineering. *Tissue Eng. Part A* **16**, 1291–1301 (2010).
18. K. D. Allen, K. A. Athanasiou, Viscoelastic characterization of the porcine temporomandibular joint disc under unconfined compression. *J. Biomech.* **39**, 312–322 (2006).
19. W. S. Vanden Berg-Foels, In situ tissue regeneration: Chemoattractants for endogenous stem cell recruitment. *Tissue Eng. Part B Rev.* **20**, 28–39 (2014).
20. J. R. Munoz, B. R. Stoutenger, A. P. Robinson, J. L. Spees, D. J. Prockop, Human stem/progenitor cells from bone marrow promote neurogenesis of endogenous neural stem cells in the hippocampus of mice. *Proc. Natl. Acad. Sci. U.S.A.* **102**, 18171–18176 (2005).
21. T. A. Partridge, J. E. Morgan, G. R. Coulton, E. P. Hoffman, L. M. Kunkel, Conversion of mdx myofibres from dystrophin-negative to -positive by injection of normal myoblasts. *Nature* **337**, 176–179 (1989).
22. M. M. Martino, P. S. Briquez, A. Ranga, M. P. Lutolf, J. A. Hubbell, Heparin-binding domain of fibrin(ogen) binds growth factors and promotes tissue repair when incorporated within a synthetic matrix. *Proc. Natl. Acad. Sci. U.S.A.* **110**, 4563–4568 (2013).
23. T. A. Holland, A. G. Mikos, Advances in drug delivery for articular cartilage. *J. Control. Release* **86**, 1–14 (2003).
24. K. Kim, J. Lam, S. Lu, P. P. Spicer, A. Lueckgen, Y. Tabata, M. E. Wong, J. A. Jansen, A. G. Mikos, F. K. Kasper, Osteochondral tissue regeneration using a bilayered composite hydrogel with

modulating dual growth factor release kinetics in a rabbit model. *J. Control. Release* **168**, 166–178 (2013).
25. M. Horie, M. D. Driscoll, H. W. Sampson, I. Sekiya, C. T. Caroom, D. J. Prockop, D. B. Thomas, Implantation of allogenic synovial stem cells promotes meniscal regeneration in a rabbit meniscal defect model. *J. Bone Joint Surg. Am.* **94**, 701–712 (2012).
26. M. Horie, I. Sekiya, T. Muneta, S. Ichinose, K. Matsumoto, H. Saito, T. Murakami, E. Kobayashi, Intra-articular injected synovial stem cells differentiate into meniscal cells directly and promote meniscal regeneration without mobilization to distant organs in rat massive meniscal defect. *Stem Cells* **27**, 878–887 (2009).
27. E. Kon, G. Filardo, M. Tschon, M. Fini, G. Giavaresi, L. Marchesini Reggiani, C. Chiari, S. Nehrer, I. Martin, D. M. Salter, L. Ambrosio, M. Marcacci, Tissue engineering for total meniscal substitution: Animal study in sheep model—Results at 12 months. *Tissue Eng. Part A* **18**, 1573–1582 (2012).
28. T. Yamasaki, M. Deie, R. Shinomiya, Y. Yasunaga, S. Yanada, M. Ochi, Transplantation of meniscus regenerated by tissue engineering with a scaffold derived from a rat meniscus and mesenchymal stromal cells derived from rat bone marrow. *Artif. Organs* **32**, 519–524 (2008).
29. H. Zhang, P. Leng, J. Zhang, Enhanced meniscal repair by overexpression of hIGF-1 in a full-thickness model. *Clin. Orthop. Relat. Res.* **467**, 3165–3174 (2009).
30. D. H. Lee, C. H. Sonn, S. B. Han, Y. Oh, K. M. Lee, S. H. Lee, Synovial fluid $CD34^{-}$ $CD44^{+}$ $CD90^{+}$ mesenchymal stem cell levels are associated with the severity of primary knee osteoarthritis. *Osteoarthritis Cartilage* **20**, 106–109 (2012).
31. T. P. Richardson, M. C. Peters, A. B. Ennett, D. J. Mooney, Polymeric system for dual growth factor delivery. *Nat. Biotechnol.* **19**, 1029–1034 (2001).
32. P. R. Tata, H. Mou, A. Pardo-Saganta, R. Zhao, M. Prabhu, B. M. Law, V. Vinarsky, J. L. Cho, S. Breton, A. Sahay, B. D. Medoff, J. Rajagopal, Dedifferentiation of committed epithelial cells into stem cells in vivo. *Nature* **503**, 218–223 (2013).
33. N. Ozeki, T. Muneta, H. Koga, H. Katagiri, K. Otabe, M. Okuno, K. Tsuji, E. Kobayashi, K. Matsumoto, H. Saito, T. Saito, I. Sekiya, Transplantation of Achilles tendon treated with bone morphogenetic protein 7 promotes meniscus regeneration in a rat model of massive meniscal defect. *Arthritis Rheum.* **65**, 2876–2886 (2013).
34. B. Shen, A. Wei, S. Whittaker, L. A. Williams, H. Tao, D. D. Ma, A. D. Diwan, The role of BMP-7 in chondrogenic and osteogenic differentiation of human bone marrow multipotent mesenchymal stromal cells in vitro. *J. Cell. Biochem.* **109**, 406–416 (2010).
35. M. Singh, C. P. Morris, R. J. Ellis, M. S. Detamore, C. Berkland, Microsphere-based seamless scaffolds containing macroscopic gradients of encapsulated factors for tissue engineering. *Tissue Eng. Part C Methods* **14**, 299–309 (2008).
36. T. Zantop, A. K. Eggers, V. Musahl, A. Weimann, W. Petersen, Cyclic testing of flexible all-inside meniscus suture anchors: Biomechanical analysis. *Am. J. Sports Med.* **33**, 388–394 (2005).

Acknowledgments: We thank R. Burdie, J. Cross, F. Guo, and J. Melendez for administrative, technical, and animal care assistance. **Funding:** NIH grants AR065023 and EB009663 to J.J.M., grants from Arthroscopy Association of North America and American Orthopaedic Society for Sports Medicine to S.A.R., and a Harry M. Zweig Foundation grant to L.A.F. **Author contributions:** C.H.L. was responsible for the technical design and primary technical undertaking, and conducted the experiments, collected and analyzed data, and drafted the manuscript. S.A.R. contributed to the surgical design and animal model, performed all animal surgeries, and edited the manuscript. L.A.F. participated in surgical design, animal surgeries, and post-op animal care, and edited the manuscript. C.L. and C.E. assisted in surgery preparation and animal surgeries. J.J.M. conceived and designed the experiments, oversaw the collection of results and data interpretation, and wrote the manuscript. **Competing interests:** J.J.M. and C.H.L. hold a patent on meniscus regeneration using biomaterial scaffolds and/or small-molecule cues. **Data and materials availability:** All raw data will be available per NIH policy.

Submitted 3 June 2014
Accepted 13 November 2014
Published 10 December 2014
10.1126/scitranslmed.3009696

Citation: C. H. Lee, S. A. Rodeo, L. A. Fortier, C. Lu, C. Erisken, J. J. Mao, Protein-releasing polymeric scaffolds induce fibrochondrocytic differentiation of endogenous cells for knee meniscus regeneration in sheep. *Sci. Transl. Med.* **6**, 266ra171 (2014).

Science Translational Medicine
AAAS

Protein-releasing polymeric scaffolds induce fibrochondrocytic differentiation of endogenous cells for knee meniscus regeneration in sheep

Chang H. Lee *et al.*

Sci Transl Med **6**, 266ra171 (2014);
DOI: 10.1126/scitranslmed.3009696

Editor's Summary

Bioprinting Cartilage Scaffolds

Weak in the knees? You may need more cartilage. Because donor cartilage as well as synthetic products are scarce, Lee *et al.* devised a way to regenerate the knee meniscus, using the native tissue from sheep knees as inspiration. The authors three-dimensionally (3D) printed poly- ε-caprolactone (PCL) scaffolds based on the anatomically correct dimensions of the native meniscus. These scaffolds were loaded at specific locations with polymeric microspheres containing one of two growth factors, to be released sequentially. Connective tissue growth factor (CTGF) was released first, followed by transforming growth factor–β3 (TGFβ3). Control over both spatial and temporal protein release allowed for zone-specific matrix development: type I collagen in the outer zone and type II collagen in the inner zone, similar to the native meniscus. It is believed that such growth factor release induced endogenous stem cells to differentiate into fibrochondrocytes—the cells that make up the meniscus. In vivo in a large animal (sheep) model, the implanted scaffolds led to tissue regeneration with desired mechanical properties. If translated to humans, this acellular biomaterial would fulfill the major unmet need of repairing deteriorated cartilage in not only the knees but also tendon-bone junctions, the intervertebral discs of the spine, and the temporomandibular joint.

Science Translational Medicine (print ISSN 1946-6234; online ISSN 1946-6242) is published weekly, except the last week in December, by the American Association for the Advancement of Science, 1200 New York Avenue NW, Washington, DC 20005.